Korean J. Chem. Eng., 37(2), 322-331 (2020)
DOI: 10.1007/s11814-019-0443-3

pISSN: 0256-1115
eISSN: 1975-7220

Study on the feasibility of using a pilot plant Scheibel extraction column for the extraction and separation of lanthanum and cerium from aqueous solution

Mehdi Asadollahzadeh†, Rezvan Torkaman, and Meisam Torab-Mostaedi

Materials and Nuclear Fuel Research School, Nuclear Science and Technology Research Institute,
P. O. Box: 11365-8486, Tehran, Iran
(*Received 11 July 2019 • accepted 1 December 2019*)

Abstract−Batch and continuous experiments were carried out in a Scheibel extraction column to separate La(III) from Ce(III). Central composite design was used to evaluate the influence of pH, extractant concentration in the batch experiments, and the influence of rotor speed, phase flow rates in the continuous experiments. At optimum conditions (pH 3.5, D2EHPA extractant concentration 0.05 M, rotor speed 128 rpm, dispersed phase flow rate 32 L/h and continuous phase flow rate 18 L/h), high extraction efficiency and separation factor equal to 88.12% and 4.89, respectively, for cerium separation from lanthanum were reasonably well predicted by the model. At higher rotor speed, La(III) and Ce(III) ions move faster from aqueous to the organic phase, which retards the higher interaction between ions and D2EHPA extractant. The results showed that this extraction column could be a potential candidate for the extraction and separation of La(III) and Ce(III) ions or other industrial wastewater.

Keywords: Rare Earth, Scheibel Column, Slip Velocity, Dispersed Phase Holdup

INTRODUCTION

The widespread use of rare earth elements (REE) has increased in various sectors of industry, automotive, and high-tech equipment [1]. For example, lanthanum is used in the lamp industry, and projectors, hybrid batteries, alloying agents for iron, steel and catalyst components, and cerium is used in the glass industry, alloy production, catalyst and hydrogen storage [1,2]. Simultaneously, increasing demand for rare earth production has become an issue worldwide. Thus, there is considerable interest in developing and using effective extraction and separation processes for rare earth production. The solvent extraction process has attracted more attention as an effective method for the extraction and separation of rare earth elements [3]. It is considered to be a feasible and an alternative technique, compared to the other purification techniques such as ion exchange [4,5], precipitation [6] and crystallization [7] processes, owing to its ease of operation and high efficiency. Also, the complex formation between ions and extractant molecules in this method has a high potential for complete and selective extraction of the rare earth element ions [1].

Extractant solvents such as D2EHPA [8-10], EHEHPA [8,11], PC88A [12], Cyanex 272 [9,13], Cyanex 301 [14], Cyanex 921 and Cyanex 923 [15], Aliquat 336 [16], Alamine 336 [16,17], Tri-n-octylamine (TOA) [18,19], 8-hydroxyquinoline [20], *sec*-octylphenoxy acetic acid [21] have been investigated by several researchers. Among them, organophosphorus extractant or cation exchangers such as D2EHPA and EHEHPA are considered to be the best extractants for extraction and separation of rare earth elements, owing to their affinity for the separation of all rare earth ions [1].

In addition to the effect of solvent, the equipment also plays an important role in the performance of the process. Different equipment is used in the solvent extraction process, but the usual equipment is a battery of mixer-settlers, which REE separation processes in the industrial scale are all done in this equipment [22]. But, the single-stage mixer-settler does not have the proper performance in countercurrent flows, and it is necessary to increase the number of stages to reach 99.99% purity, which in some cases requires more than 100 stages to achieve high purity for rare earth metals. In comparison to mixer-settlers, the pulsed [23,24] and agitated extraction columns such as rotating impeller column [25], Oldshue-Rushton column [26] and Scheibel column provide an effective and highly satisfactory way for the purification of a liquid or the recovery of components from aqueous solutions [27]. These columns are capable of handling large throughputs to any desired degree of efficiency in both small and large scale operations [28,29].

The Scheibel extraction column is an agitated extraction column consisting of a mixing zone containing a flat-bladed turbine-type agitator and a calming zone containing a wire-mesh or structured packing [28]. The first Scheibel column with seven mixer-settler stages was utilized in large commercial scale in 1946; it was obvious that new liquid extraction processes were needed, particularly with a large number of theoretical stages. Different designs have been proposed for the Scheibel column, and three generations of these columns have been reported in the literature [30,31]. The design of this column requires the experience in determining the main dimensions, including diameter and height, and the packing and mixing sections. The volumetric flow rates and the maximum allowable linear velocities of the phases are required for the determination of diameter [28]. The dispersed phase holdup and characteristic velocity have an important role in defining maximal allowable linear

†To whom correspondence should be addressed.
E-mail: masadollahzadeh@aeoi.org.ir

velocities that are highly studied in the literature due to their importance in extraction columns [32-38].

Despite the importance of these parameters, studies regarding them in the Scheibel column have not been reported in the literature. In addition, the efficiency and feasibility of using this column in the extraction and separation of rare earth elements has not been investigated in the literature.

Therefore, the extraction and separation of lanthanum and cerium ions from aqueous solution, the study of changes in the dispersed phase holdup and slip velocity in the pilot plant Scheibel column were investigated in this paper. The effect of operating parameters was investigated by using the design of the experiments, and the materials were selected as feed for the column based on the investigation and optimization of the main parameters on the batch experimental section.

EXPERIMENTAL

1. Materials Used

Of the dispersed solvents, kerosene and D2EHPA extractant were supplied by petroleum refinery Tehran and Aldrich company, respectively. The physical properties of these solvents are shown in Table 1, the aqueous solution containing lanthanum nitrate (150 ppm) and cerium nitrate (150 ppm) dissolved in distilled water with specific acidity was used as the continuous phase.

2. Description of the Apparatus

The original Scheibel column consisted of an inner diameter of 113 mm, the height of 1,430 mm, the ten mixing sections and eleven structured packing sections. The length of the impeller was 23.5 mm, and the internals was AISI 316 stainless steel with Teflon seals. A settler of 168 mm diameter at each end of the column

Table 1. Physical properties of the organic and aqueous phases used in the pilot column

	ρ (kg·m^{-3})	μ ($\times 10^3$ kg·m^{-1}s^{-1})	σ ($\times 10^3$ N/m)
Continuous phase	1019	0.9894	16.4
Dispersed phase	885	1.4245	

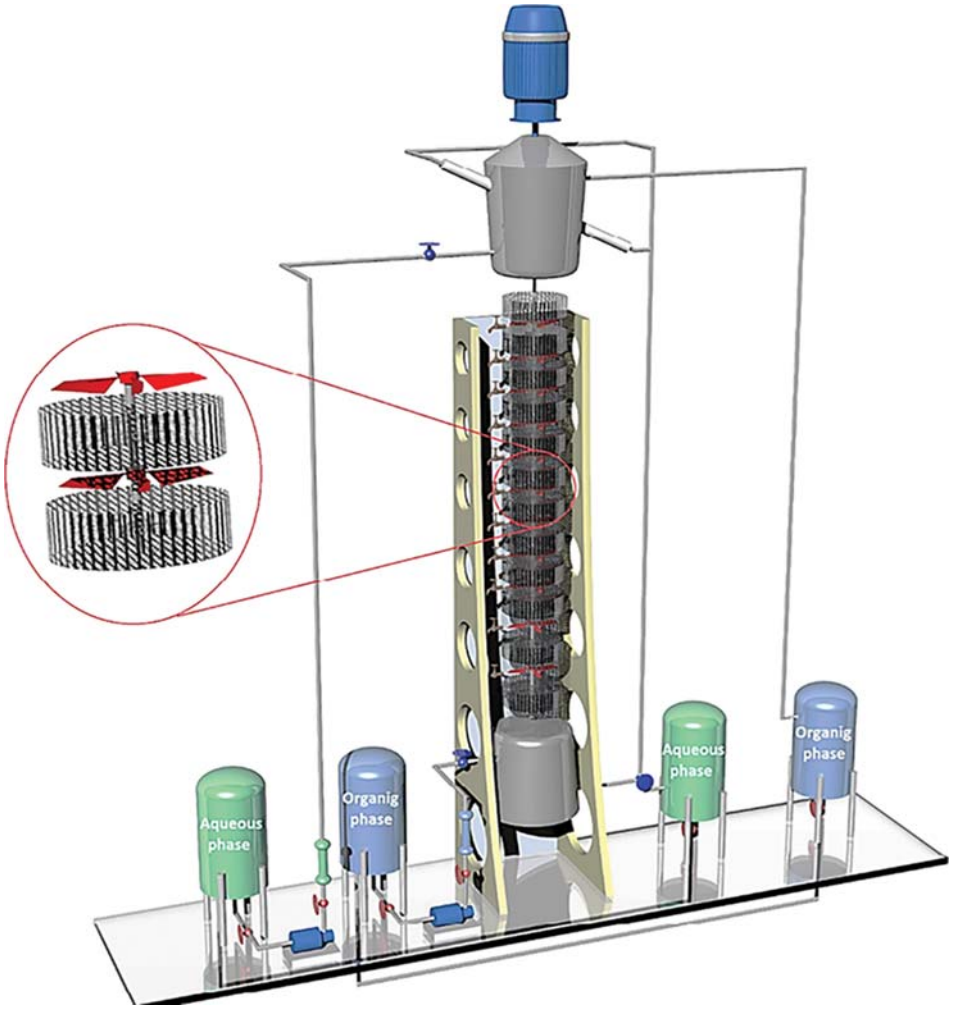

Fig. 1. Schematic of pilot plant Scheibel extraction column.

permitted the liquids to coalesce and decant separately. A solenoid valve (a normally closed type) was provided at the outlet stream of the heavy phase for controlling the interface location. A schematic diagram of the experimental apparatus is described in Fig. 1.

3. Design of Experiments

In the batch section, we used experimental variables such as the initial aqueous pH, D2EHPA extractant concentration to design the experiments. The obtained results we analyzed by utilizing the central composite design (CCD) method. Although, the other parameters such as the initial concentration of cerium (Ce), lanthanum (La) and the organic to aqueous phase ratio (O/A) might be important, these factors were ignored. Therefore, all the experiments were carried out with 150 ppm of lanthanum and cerium ions and equal phase of two phases in the ambient temperature. A central composite design with 13 runs and five replicates of the central points was carried out to determine the optimum values for maximum efficiency for cerium ions and the maximum separation factor.

In the continuous section, the data evaluation for the dispersed phase holdup, slip velocity, and extraction efficiency was performed according to the central composite design method with 20 runs and six replicates of the central points. The main operating parameters in the experiments were rotor speed, dispersed and continuous phase flow rates that the range and the levels of the variables are described in Table 2.

4. Determination of Extraction Efficiency and Separation Factor

The concentration of metal ions in the aqueous phase was determined by inductively coupled plasma atomic emission spectroscopy (ICP-AES), and the concentration of metal ions in the organic phase was calculated by the mass balance method. Therefore, the extraction efficiency (E), is calculated as follows:

$$E(\%) = \frac{[C]_{total} - [C]_{aq}}{[C]_{total}} \times 100 \quad (1)$$

The distribution ratio (D) and separation factor (β) were calculated by Eqs. (2) and (3) as follows:

$$D = \frac{[C]_{org}}{[C]_{aq}} \quad (2)$$

$$\beta = \frac{D_{Ce}}{D_{La}} \quad (3)$$

where $[C]_{org}$, $[C]_{aq}$ and $[C]_{total}$ denote the metal concentration in the organic, aqueous phases in the equilibrium condition and total concentration in the aqueous phase, respectively.

5. Determination of Dispersed Phase Holdup and Slip Velocity

Hold-up measurement involved operating the column under the desired steady-state conditions and then rapidly closing the inlet and outlet valves. After the agitator was stopped and time allowed for complete phase separation, the dispersed phase was permitted to disengage from the interface on the top of the extraction column. After 10-15 min, the variation in the interface height between operation and after settling was determined and then converted into the corresponding volume to estimate the holdup. The slip velocity is calculated by the sum of the actual linear velocities of the dispersed and continuous phases based on the variation in the dispersed phase holdup.

Table 2. Range and the levels of variables in the continuous experiments

Variable	Name	$-\alpha$	-1	0	+1	$+\alpha$
Rotor speed (rpm)	N	75	95	115	135	155
Continuous phase flow rate (L/h)	Q_c	18	24	30	36	42
Dispersed phase flow rate (L/h)	Q_d	18	24	30	36	42

Table 3. Design matrixes and responses for extraction efficiency (%E) and separation factor (SF) in the batch experiments

Run	D2EHPA extractant concentration	pH	Experimental data			Predicted data from models by central composite design method		
			E%_La	E%_Ce	SF	E%_La	E%_Ce	SF
1	0.055	4	58.56	78.52	2.59	58.61	79.09	2.67
2	0.055	4	57.14	79.48	2.91	58.61	79.09	2.67
3	0.01	4	9.23	18.65	2.25	8.90	14.60	1.97
4	0.055	4	59.12	78.88	2.58	58.61	79.09	2.67
5	0.023	6.12	19.82	25.46	1.38	23.43	33.44	1.72
6	0.1	4	87.65	94.53	2.43	80.85	89.65	2.58
7	0.055	4	59.12	79.46	2.68	58.61	79.09	2.67
8	0.055	1	14.52	21.26	1.59	14.60	22.64	1.37
9	0.023	1.88	8.25	11.56	1.45	6.79	11.35	1.67
10	0.055	7	65.89	80.25	2.10	58.67	69.95	1.72
11	0.087	1.88	40.12	52.75	1.67	43.45	53.37	1.90
12	0.087	6.12	80.56	89.23	2.00	89.10	98.15	2.35
13	0.055	4	59.12	79.13	2.62	58.61	79.09	2.67

RESULTS AND DISCUSSION

1. Optimization Parameters in Batch Experimental Section

The significance of the main interaction of two independent variables, D2EHPA extractant concentration (X1), and initial aqueous pH (X2), into five levels with the responses for extraction efficiencies (%E) of La(III) and Ce(III), separation factor (SF), and the results from predicted models is presented in Table 3. The results of this table show that two variables have significant effects on the separation factor and they are necessary to optimize before using the solution as the feed into the Scheibel column for continuous experiments.

The final equation in terms of the actual factors for lanthanum extraction efficiency (Y_1(%)), cerium extraction efficiency (Y_2(%)), and separation factor (Y_3(-)) and independent variables is expressed in the following:

$$Y_{1\text{ or }2\text{ or }3}=C_1+C_2X_1+C_3X_2+C_4X_1X_2+C_5X_1^2+C_6X_2^2 \quad (4)$$

The constant parameters for the prediction of extraction efficiency and separation factor are shown in Table 4. Among different models, the quadratic model was found to be the best fit model for responses in the batch experiments.

Table 4. Constant parameters in the predicted equation (Eq. (4)) for determination of extraction efficiency (E%_La and E%_Ce) and separation factor (SF)

Constant parameters	Y_1 E%_La	Y_2 E%_Ce	Y_3 SF
C_1	−50.808	−78.502	−0.193
C_2	1118.113	1964.137	22.172
C_3	20.997	32.441	0.975
C_4	106.925	83.629	1.481
C_5	−6784.938	−13316.173	−193.827
C_6	−2.442	−3.644	0.124

The variation of extraction efficiency with the initial aqueous pH and D2EHPA extractant concentration in 3D plots and contour plots is shown in Figs. 2 and 3 for Ce(III) or La(III) extraction. In addition, the standard error for prediction of extraction efficiency according to the quadratic model is shown in Fig. 4.

As shown in Fig. 2 and 3, the variation in extraction efficiency for both metal ions was directly related to the pH of initial aqueous. D2EHPA extractant is an acidic extractant, and its reaction with rare earth elements releases hydrogen ions. Therefore, the intensification of aqueous phase acidity decreases the extraction efficiency with the reversing the equilibrium reaction between D2EHPA extractant and two metal ions. In addition, the extraction rate increases with the increase in the D2EHPA extractant concentration at all values for initial aqueous pH. But, in the high values for this parameter, there is a slight increase in the extraction efficiency.

The higher concentration of D2EHPA extractant leads to more complex formation, but in higher concentrations, the amount of free metal ions decreases and the rate of complex formation de-

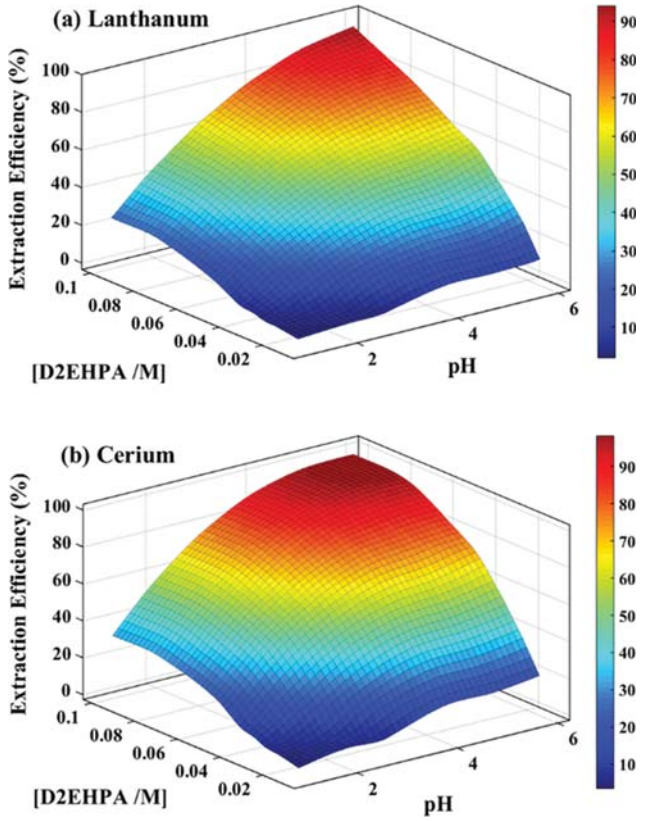

Fig. 2. 3D plots for extraction efficiency as a function of initial aqueous pH and D2EHPA extractant concentration (25 °C, O/A ratio equal to 1, [La]=[Ce]=150 ppm).

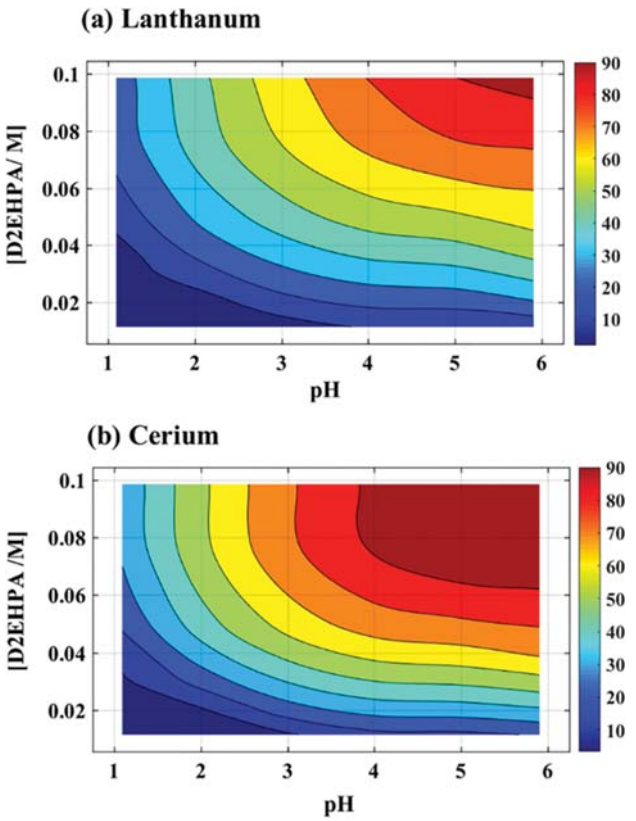

Fig. 3. Contour plots for extraction efficiency as a function of initial aqueous pH and D2EHPA extractant concentration (25 °C, O/A ratio equal to 1, [La]=[Ce]=150 ppm).

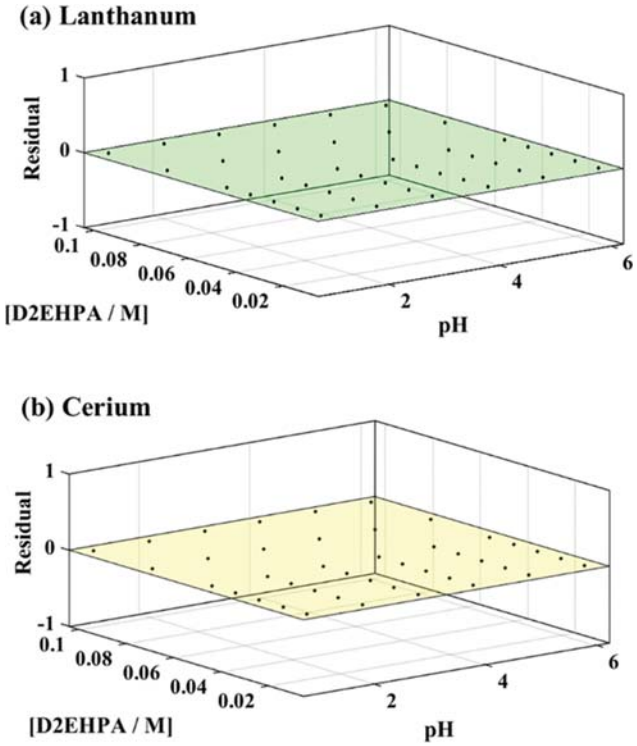

Fig. 4. Standard errors from the predicted models for extraction efficiency as a function of initial aqueous pH and D2EHPA extractant concentration (25 °C, O/A ratio equal to 1, [La]=[Ce]= 150 ppm).

creases, so the increment in the extraction efficiency will gradually change with the higher value for D2EHPA extractant.

Fig. 5 illustrates the effects of initial aqueous pH and D2EHPA extractant concentration on the separation factor with contour and residual plots. It can be seen from Fig. 5 that an increase in the initial aqueous pH from 2 to 3.5-4 increases the separation factor, but higher values are not desirable for the separation of the two ions. The reduction in the separation factor is related to the increase in the distribution ratio of both metals (see in Eq. (2)). A further increment in distribution ratio of La(III) in comparison with the value for Ce(III) (see in Eq. (3)) causes a decrement in the separation factor (SF).

The same result applies to the concentration of D2EHPA extractant. The enhancement in the concentration up to 0.05 M leads to an increase in the separation factor, but higher values are not suitable, and the reduction of the separation factor is obtained by increasing the distribution ratio of both metals.

According to Fig. 5, the value of R^2 for the predicted model equal to 0.8911 and adjusted R^2 equal to 0.8214, good agreement between the model and the experimental data was observed in the batch experiments. The optimum conditions with the desirability of 1 were obtained equal to 3.5 and 0.05 M for pH, and D2EHPA extractant concentration, respectively, by using the statistical optimization in the software.

2. Optimization Parameters in Continuous Experimental Section

2-1. Extraction Efficiency and Separation Factor

Response surface methodology (RSM) was used for improving

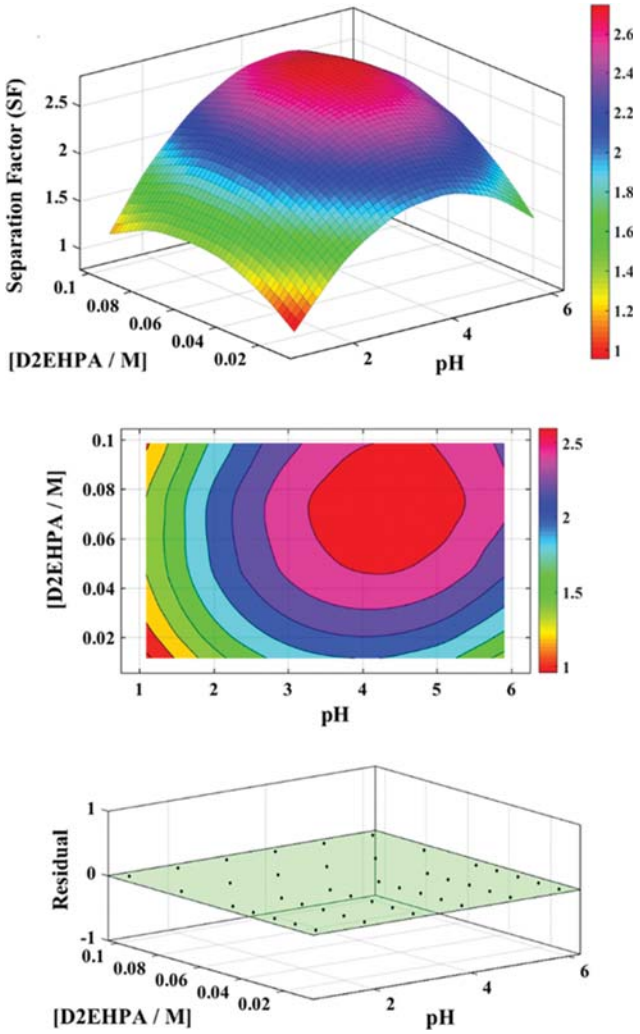

Fig. 5. 3D, contour, and residual plots for separation factor as a function of initial aqueous pH and D2EHPA extractant concentration (25 °C, O/A ratio equal to 1, [La]=[Ce]=150 ppm).

the optimization and evaluation of the interaction of variables such as rotor speed, dispersed phase flow rate and continuous phase flow rate on the extraction efficiencies of lanthanum, cerium and separation factor. The three-dimensional surface response plots of these interactions are shown in Figs. 6, 7, and 8.

Fig. 6 represents the interaction of rotor speed with continuous phase flow rate on the E%_La, E%_Ce, and separation factor. The extraction efficiency for lanthanum, cerium, and separation factor increases with the enhancement in the rotor speed due to its high specific surface area from the droplet breakage. The enhancement in the surface area causes the required surface between the two phases increases, which increments the mass transfer rate between both phases for reaction and complex formation.

In addition, the separation factor increases with the increase in the rotor speed. The effect of the continuous phase flow rate in the different rotor speed shows the increase in the extraction efficiency for lanthanum and cerium, but this parameter has the reverse effect in the low rotor speed with the reduction in the separation factor, but during the high value for agitation, the increase of the separa-

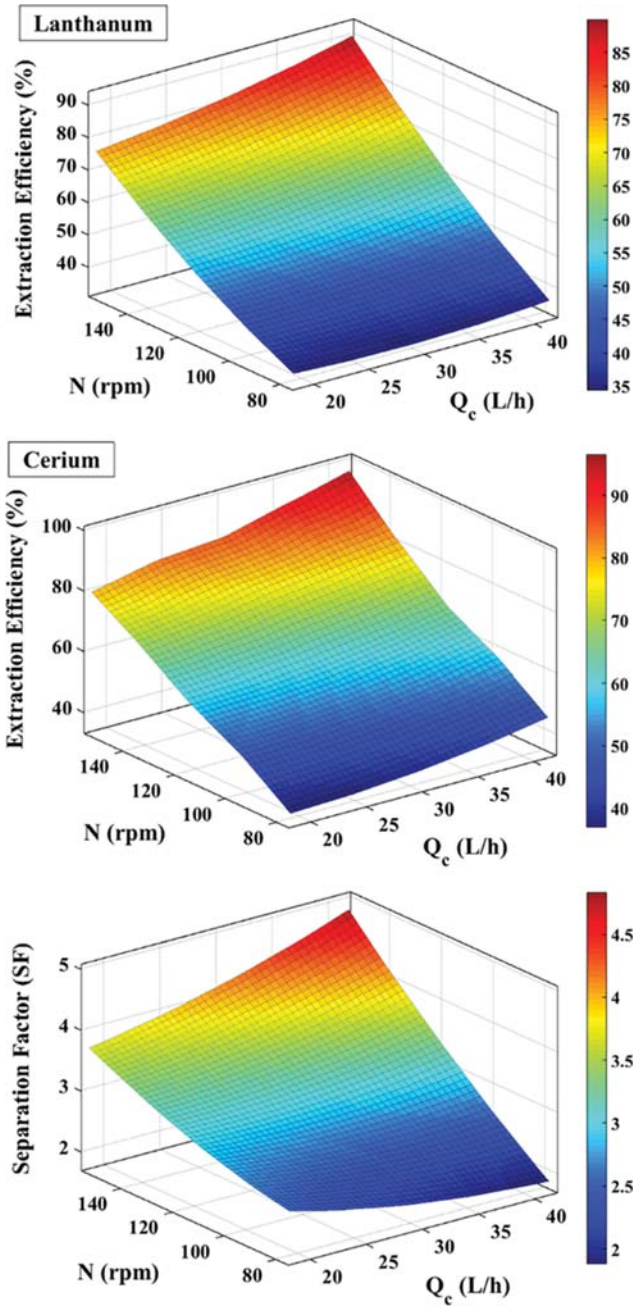

Fig. 6. 3D plots for extraction efficiency and separation factor as a function of rotor speed and continuous phase flow rate (25 °C, Q_d=30 L/h).

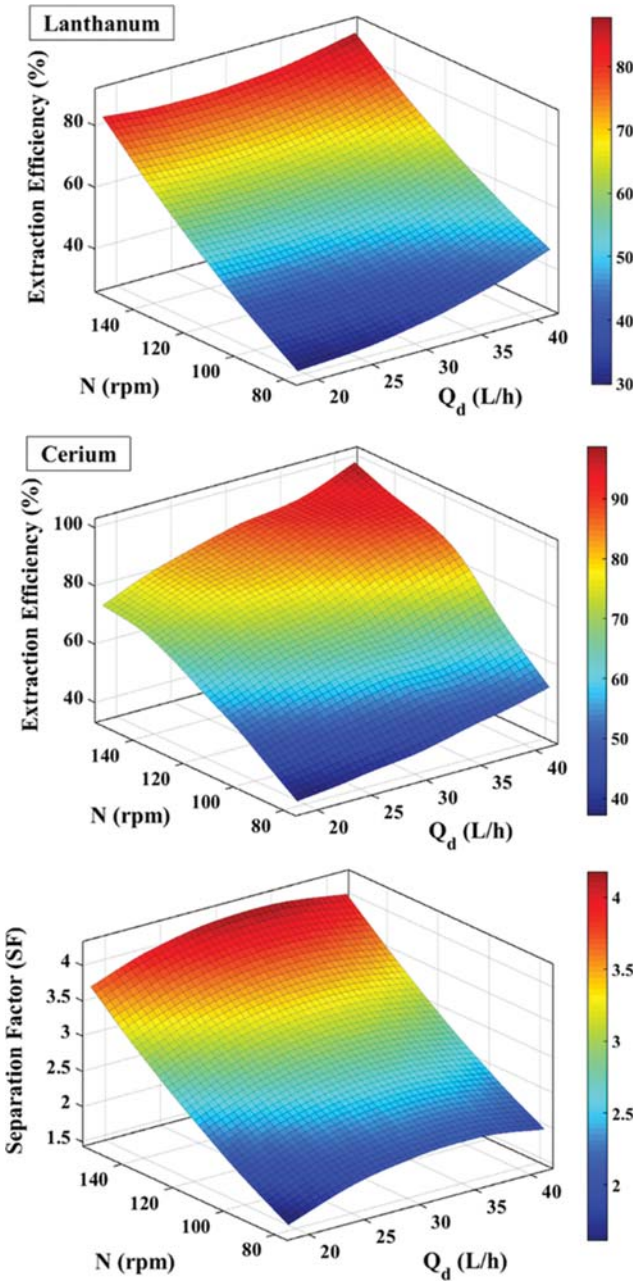

Fig. 7. 3D plots for extraction efficiency and separation factor as a function of rotor speed and dispersed phase flow rate (25 °C, Q_c=30 L/h).

tion factor has been observed in Fig. 6. These variations are related to the increase or decrease of the distribution ration of the two ions, which causes the change in the separation factor.

The results of the interaction between N and Q_d in Fig. 7 show that both parameters have positive effects on the extraction efficiency and separation factor; the increase of E%_La or E%_Ce and separation factor is observed with the increase of these parameters, but the amount of variation in direction of axis of Q_d in all values of rotor speed is less than the variation in the agitation speed. By increasing the flow rate of the dispersed phase, more droplets enter the column, and the possibility of reaction with more metal ions will be provided due to the increment in the reaction surface.

The effects of phase flow rates on the extraction efficiency, according to Fig. 8 show the desirability of high values for E%_La or E%_Ce.

Turbulent flow due to an increase in Q_c does not have a positive effect on the amount of separation factor since it reduces the probability of necessary reactions between droplets and aqueous phase. However, the reduction of separation factor with high continuous phase flow rate indicates that a limited increase in these parameters is required to reach the maximum separation factor.

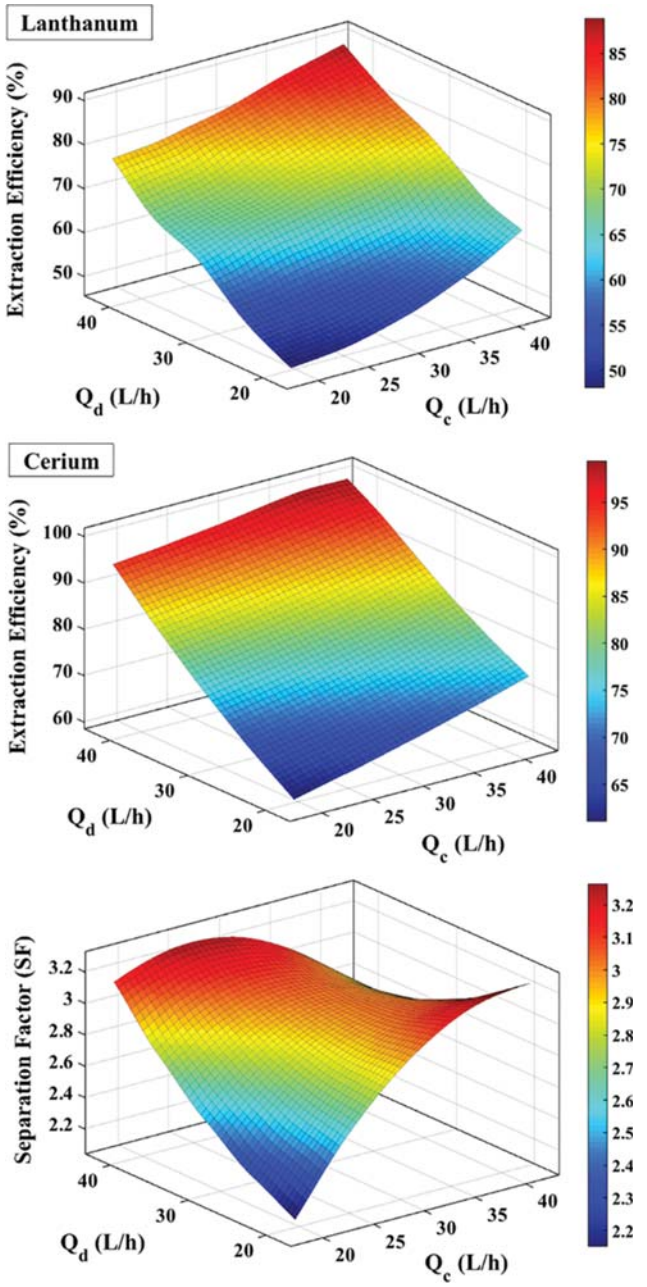

Fig. 8. 3D plots for extraction efficiency and separation factor as a function of continuous and dispersed phase flow rates (25 °C, N=115 rpm).

The second-order polynomial was used to explain the interaction between the extraction efficiency and separation factor for lanthanum and cerium:

$$Y_{1\text{ or }2\text{ or }3}=C_1+C_2N+C_3Q_c+C_4Q_d+C_5NQ_c+C_6NQ_d+C_7Q_cQ_d+C_8N^2+C_9Q_c^2+C_{10}Q_d^2 \quad (5)$$

where N, Q_d, Q_c are the rotor speed, dispersed phase flow rate, and continuous phase flow rate, respectively.

The constant parameters for the prediction of extraction efficiencies for lanthanum, cerium, and separation factor are shown in Table 5. The ANOVA table (Table 6) shows that Eq. (5) is significant

Table 5. Constant parameters in the predicted equation (Eq. (5)) for determination of extraction efficiency (E%_La and E%_Ce) and separation factor (SF)

Constant parameters	Y_1 E%_La	Y_2 E%_Ce	Y_3 SF
C_1	13.474	−51.358	0.021
C_2	0.077	1.432	−0.023
C_3	−0.662	−0.845	−0.073
C_4	0.027	1.240	0.230
C_5	7.955×10^{-3}	5.215×10^{-3}	9.870×10^{-4}
C_6	-5.981×10^{-3}	-5.775×10^{-3}	-2.946×10^{-5}
C_7	−0.020	−0.012	-2.798×10^{-3}
C_8	2.035×10^{-3}	-3.771×10^{-3}	8.986×10^{-5}
C_9	0.011	0.014	8.943×10^{-4}
C_{10}	0.029	3.546×10^{-3}	-2.126×10^{-3}

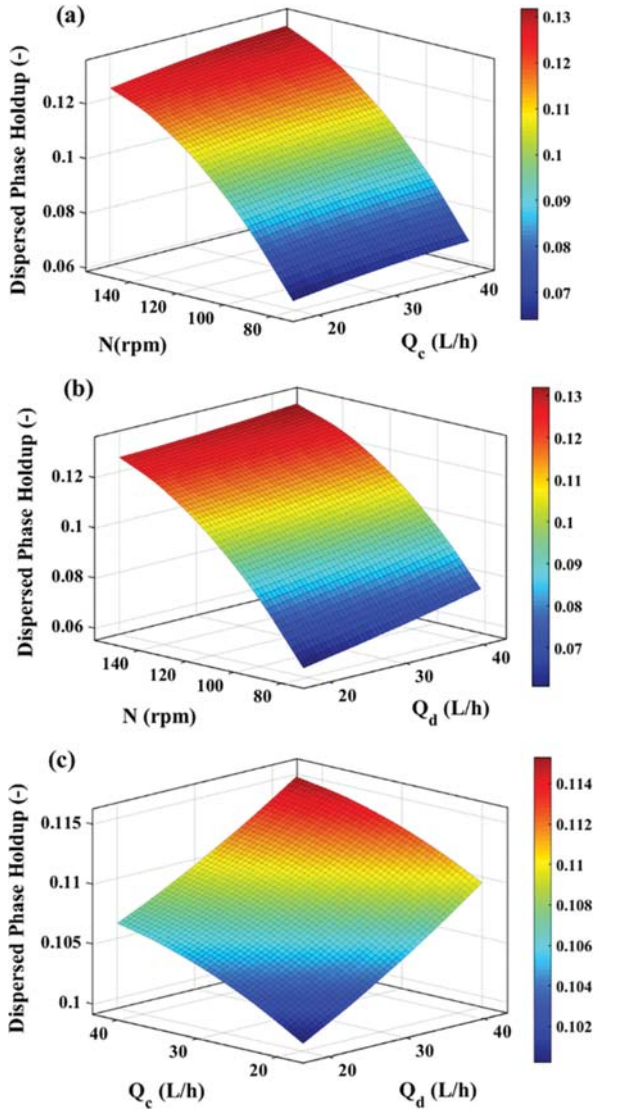

Fig. 9. 3D plots for dispersed phase holdup as a function of (a) rotor speed and continuous phase flow rate (Q_d=30 L/h); (a) rotor speed and dispersed phase flow rate (Q_c=30 L/h); (c) dispersed and continuous phase flow rates (N=115 rpm).

Table 6. Analysis of variance (ANOVA) for prediction of extraction efficiency for lanthanum and cerium

Source	Extraction efficiency for lanthanum				Extraction efficiency for cerium			
	Sum of squares	Degree freedom	F-value	P-value	Sum of squares	Degree freedom	F-value	P-value
Model	3120.59	9	14.27	0.0001	2577.21	9	23.81	<0.0001
X_1-N	2819.58	1	116.08	<0.0001	2315.17	1	192.47	<0.0001
X_2-Q_c	71.60	1	2.95	0.1168	35.22	1	2.93	0.1179
X_3-Q_d	150.69	1	6.20	0.0320	130.85	1	10.88	0.0080
X_1X_2	14.58	1	0.60	0.4564	6.27	1	0.52	0.4870
X_1X_3	8.24	1	0.34	0.5731	7.68	1	0.64	0.4427
X_2X_3	8.45	1	0.35	0.5685	2.90	1	0.24	0.6338
X_1^2	19.10	1	0.79	0.3961	65.60	1	5.45	0.0417
X_2^2	4.70	1	0.19	0.6693	7.07	1	0.59	0.4611
X_3^2	31.11	1	1.28	0.2842	0.47	1	0.039	0.8473
Residual	242.90	10	-	-	120.29	10	-	-
Lack of fit	157.56	5	1.85	0.2587	64.88	5	1.17	0.4333
Pure error	85.35	5	-	-	55.40	5	-	-
Cor total	3363.49	19	-	-	2697.49	19	-	-
R-squared	0.9278	-	-	-	0.9554	-	-	-
Adj R-squared	0.8628	-	-	-	0.9153	-	-	-
Pred R-squared	0.6013	-	-	-	0.7734	-	-	-

from the model F-value of 14.27, 23.81, and P-value of <0.0001 for lanthanum and cerium extraction, respectively. The coefficient of determination R^2 equal to 0.9278, and 0.9554 describes the percentages of variability obtained by the predicted equations.

The optimum conditions were calculated based on the variance tests and response surface plots with the consideration of the high value for the separation factor. The results show that most desirable conditions are the rotor speed in 128 rpm, dispersed phase flow rate 32 L/h and continuous phase flow rate 18 L/h, which predicted the high extraction efficiency equal to 85.67% for Ce(II), 58.52% for La(III) and separation factor equal to 4.23. Confirmatory tests were also performed by using the optimum setting operating parameters to test the validity of the results predicted by the models. The best response or the highest separation value equal to 4.89 and extraction efficiency for cerium and lanthanum equal to 88.12% and 60.29%, respectively, was obtained to represent the accuracy and capability of the used theoretical models.

2-2. Dispersed Phase Holdup and Slip Velocity

Fig. 9(a) represents the effect of changing rotor speed and continuous phase flow rate on the dispersed phase holdup in the pilot plant Scheibel column. The trend in this graph shows that the dispersed phase holdup has been less influenced by the change in the continuous phase flow rate. But, in the constant condition for Q_c, the dispersed phase holdup increases by the increase in the rotor speed due to the reduction on the Sauter mean drop diameter by using more agitation in the column. By using the interaction between the dispersed phase flow rate and agitation speed, according to Fig. 9(b), the dispersed phase holdup increases with the increase in rotor speed and in all values for Q_d due to the high value of smaller droplets in the column. In addition, the dispersed phase holdup increases with the increase in the dispersed phase flow rate due to the availability of more droplets in the column. According to Fig. 9(c), the dispersed phase holdup is not significantly affected while changing the continuous phase flow rate in all values for Q_d. But, the increase in the dispersed phase holdup was observed by using the higher value for Q_d in all values for Q_c.

The prediction of dispersed phase holdup was reported by Houshyar and co-workers for the Scheibel extraction column with three physical systems (toluene-water, n-butyl acetate-water, n-butanol-water) [39], as follows:

$$\varphi = 1.54\left(\frac{V_d^3\rho_d}{g\mu_c}\right)^{0.23}\left(\frac{\mu_d}{\mu_c}\right)^{-0.73}\left(\frac{N^4 d^4 \rho_c}{\sigma g}\right)^{0.47}\left(1+\frac{V_d}{V_c}\right)^{-0.01} \quad (6)$$

The above correlation was obtained with 72.51% average absolute relative error for the results of lanthanum and cerium extraction. This equation was reported in non-reactive extraction condition. Therefore, a high error value is observed in the reactive condition. The same equation was reconsidered with regard to the reactive extraction data for La(III) and Ce(III) extraction. The modified equation was obtained as follows:

$$\varphi = 1.612\left(\frac{V_d^3\rho_d}{g\mu_c}\right)^{0.183}\left(\frac{\mu_d}{\mu_c}\right)^{-0.146}\left(\frac{N^4 d^4 \rho_c}{\sigma g}\right)^{0.199}\left(1+\frac{V_d}{V_c}\right)^{-0.322} \quad (7)$$

The above correlation showed a 9.33% AARE value in the prediction of the experimental results.

The 3D plot of the interaction between operating parameters for slip velocity is shown in Fig. 10. The interaction of the slip velocity with rotor speed and phase flow rates shows that the slip velocity decreased with enhancement in the higher value for agitation speed in all values for Q_c and Q_d, due to its high dispersed phase holdup. At all ranges of N, the slip velocity decreases with the increase in the Q_d due to the lower residence time for drops along the column. In addition, the slip velocity has been less influenced by the variation in the values for Q_c at all values for Q_d and N.

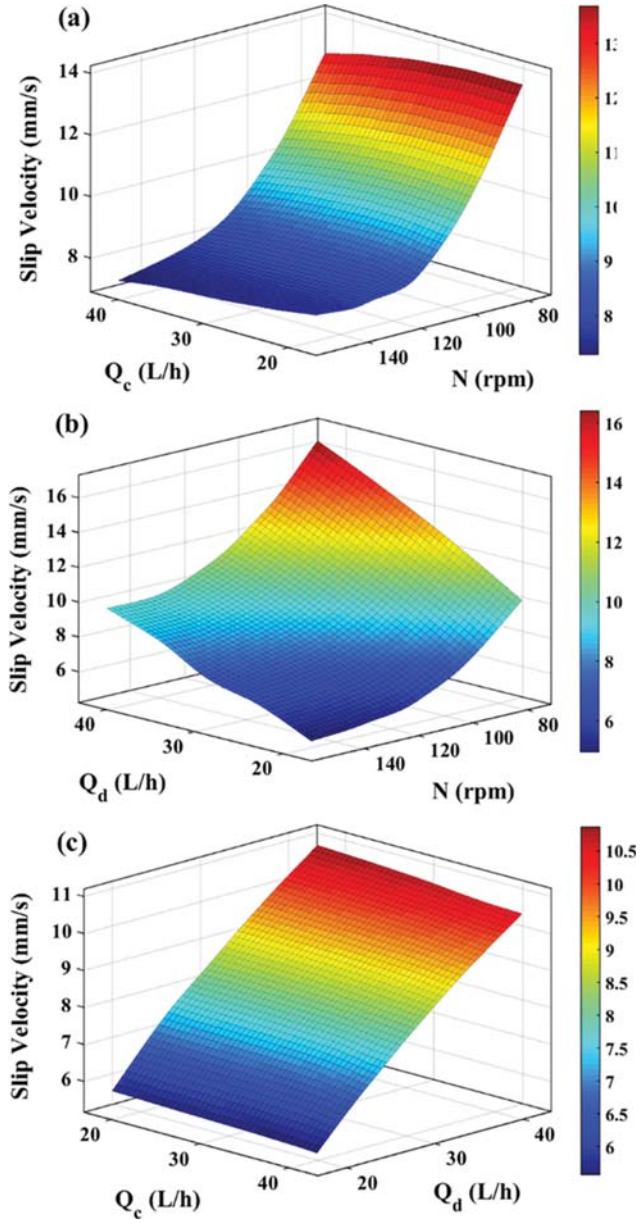

Fig. 10. 3D plots for slip velocity as a function of (a) rotor speed and continuous phase flow rate (Q_d=30 L/h); (a) rotor speed and dispersed phase flow rate (Q_c=30 L/h); (c) dispersed and continuous phase flow rates (N=115 rpm).

CONCLUSION

Response surface methodology (RSM) was valuable for modeling and optimizing the extraction and separation of cerium from lanthanum in the rare earth element separation process. To obtain the optimized conditions for the high separation factor, the experiments were designed by using CCD method in two sections (the batch experimental work and the continuous experimental work in the pilot plant Scheibel column). The separation of the cerium from lanthanum was successfully modeled with a high separation factor. Optimized conditions for operating parameters were applied experimentally in the Scheibel column and an acceptable response was achieved. The rotor speed had the most significant effect on the extraction rate for lanthanum and cerium, separation factor, dispersed phase holdup and slip velocity. A better extraction rate for La(III) and Ce(III) could be achieved at higher agitation speed. Finally, in this research, the pilot plant Scheibel column showed good performance in the extraction and separation of La(III) and Ce(III), and this could be good extraction equipment for alternative separation of rare earth elements.

NOMENCLATURE

CCD : central composite design
D : distribution ratio [-]
d : rotor diameter [m]
E : extraction efficiency [%]
N : rotor speed [s^{-1}]
Q_c : continuous phase flow rate [m^3/s]
Q_d : dispersed phase flow rate [m^3/s]
RSM : response surface methodology
SF : separation factor [-]
V_c : continuous phase velocity [m s^{-1}]
V_d : dispersed phase velocity [m s^{-1}]
V_{slip} : slip velocity [m s^{-1}]

Greek Letters

$\Delta\rho$: density difference between phases [kg m^{-3}]
β : separation factor [-]
μ : viscosity [Pa·s]
ρ : density [kg m^{-3}]
σ : interfacial tension [N m^{-1}]
φ : dispersed phase holdup [-]

Subscripts

c : continuous phase
d : dispersed phase

REFERENCES

1. D. A. Atwood, *The rare earth elements: fundamentals and application*, Wiley, New York (2016).
2. N. Krishnamurthy and C. K. Gupta, *Extractive metallurgy of rare earths*, CRC Press, New York (2016).
3. J. Zhang, B. Zhao and B. Schreiner, *Separation Hydrometallurgy of Rare Earth Elements*, Springer, New York (2016).
4. D. L. Ramasamy, S. Khan, E. Repo and Sillanpää M, *Chem. Eng. J.*, **322**, 56 (2017).
5. S. Ftekhar, V. Srivastava, S. B. Hammouda and M. Sillanpää, *Carbohydr. Polym.*, **194**, 274 (2018).
6. W. Zhang and R. Q. Honaker, *Int. J. Coal Geology*, **195**, 189 (2018).
7. X. Yin, Y. Wang, X. Bai, Y. Wang, L. Chen, C. Xiao, J. Diwu, S. Du, Z. Chai, T. E. Albrecht-Schmitt and S. Wang, *Nature Comm.*, **8**, 14438 (2017).
8. F. Zhang, W. Wu, X. Bian and W. Zeng, *Hydrometallurgy*, **149**, 238 (2014).
9. R. Habibpour, M. Dargahi, E. Kashi and M. Bagherpour, *Metall. Res. Technol.*, **115**, 207 (2018).

10. P. Ramakul, N. Leepipatpiboon, C. Yamoum, U. Thubsuang, S. Bunnak and U. Pancharoen, *Korean J. Chem. Eng.*, **26**, 765 (2009).
11. F. Jiang, S. Yin, C. Srinivasakannan, S. Li and J. Peng, *Chem. Eng. J.*, **334**, 2208 (2018).
12. K. H. Ryu, C. Lee, G. G. Lee, S. Jo and S. W. Sung, *Korean J. Chem. Eng.*, **30**, 1946 (2013).
13. E. Kashi, R. Habibpour, H. Gorzin and A. Maleki, *J. Rare Earths*, **36**, 317 (2018).
14. Abhilash, S. Sinha, M. K. Sinha and B. D. Pandey, *Inter. J. Miner. Process*, **127**, 70 (2014).
15. S. K. Sahu and S. Mishra, *Sep. Sci. Technol.*, **51**, 447 (2016).
16. R. Banda, H. S. Jeon and M. S. Lee, *Metal. Mater. Tran. B*, **45**, 2009 (2014).
17. E. Padhan and K. Sarangi, *Hydrometallurgy*, **167**, 134 (2017).
18. R. Prakorn, P. Weerawat and P. Ura, *Korean J. Chem. Eng.*, **23**, 85 (2006).
19. R. Prakorn and P. Ura, *Korean J. Chem. Eng.*, **20**, 724 (2003).
20. S. Roy, S. Basu, M. Anitha and D. K. Singh, *Korean J. Chem. Eng.*, **34**, 1740 (2017).
21. N. Song, X. Zhao, Q. Jia, W. Zhou and W. Liao, *Korean J. Chem. Eng.*, **27**, 1258 (2010).
22. F. Xie, T. A. Zhang, D. Dreisinger and F. Doyle, *Miner. Eng.*, **56**, 10 (2014).
23. G. Angelov and C. Gourdon, *Korean J. Chem. Eng.*, **32**, 37 (2015).
24. P. Amani, M. Amani and R. Hasanvandian, *Korean J. Chem. Eng.*, **34**, 1456 (2017).
25. Y. K. Lee, D. P. Ju and C. Kim, *Korean J. Chem. Eng.*, **8**, 80 (1991).
26. S. C. Lee and G. H. Hyun, *Korean J. Chem. Eng.*, **19**, 827 (2002).
27. T. C. Lo, *Commercial liquid-liquid extraction equipment*, in *Handbook of separation techniques for chemical engineers*, P. A. Schweitzer, McGraw-Hill, New York (1979).
28. J. D. Thornton, *Science and Practice of Liquid-Liquid Extraction*, Oxford University Press, Oxford (1992).
29. H. J. Bart, *Reactive Extraction*, Springer, New York (2001).
30. J. Rydberg, M. Cox, C. Musikas and G. R. Choppin, *Solvent Extraction: Principles and Practice*, Marcel Dekker, New York (2004).
31. G. M. Ritcey and A. W. Ashbrook, *Solvent extraction: principles and applications to process metallurgy*, Elsevier, New York (1984).
32. M. Asadollahzadeh, M. Torab-Mostaedi, S. Shahhosseini and A. Ghaemi, *Chem. Eng. Process*, **100**, 65 (2016).
33. R. Torkaman, M. Asadollahzadeh and M. Torab-Mostaedi, *Chem. Eng. Process*, **111**, 7 (2017).
34. M. Asadollahzadeh, M. Torab-Mostaedi and R. Torkaman, *Chem. Eng. Res. Des.*, **127**, 146 (2017).
35. M. Torab-Mostaedi, H. Jalilvand and M. Outokesh, Chem. *Ind. Chem. Eng. Q.*, **17**, 333 (2011).
36. M. Asadollahzadeh, M. Torab-Mostaedi and R. Torkaman, *Chem. Eng. Process*, **109**, 97 (2016).
37. M. Asadollahzadeh, M. Torab-Mostaedi, S. Shahhosseini and A. Ghaemi, *Chem. Eng. Res. Des.*, **105**, 177 (2016).
38. M. Asadollahzadeh, M. Torab-Mostaedi, S. Shahhosseini, A. Ghaemi and R. Torkaman, *Sep. Purif. Technol.*, **158**, 275 (2016).
39. Sh. Houshyar, M. Torab-Mostaedi and S. H. Mousavi, *J. Chem. Pet. Eng.*, **51**, 105 (2017).